Single Mol. **1** (2000) 2, 129-133



# Photonic Force Microscopy: A New Tool Providing New Methods to Study Membranes at the Molecular Level

Arnd Pralle, Ernst-Ludwig Florin, Ernst H.K. Stelzer and J. K. Heinrich Hörber

*Correspondence to*
*Cell Biology and Biophysics*
*European Molecular Biology Laboratory (EMBL)*
*Meyerhoftstrasse 1*
*D-69117 Heidelberg, Germany*
*phone +49 06221-387569*
*fax +49 06221-387306*
*email: lastname@embl-heidelberg.de*

submitted 02 May 2000
published 21 Jul 2000

## Abstract

The PFM is a three-dimensional scanning probe microscope based on optical tweezers. It evolved from AFM techniques by replacing the mechanical cantilever of the AFM with optical tweezers and the cantilever tip by a trapped bead. Various detection systems measure the three-dimensional position of the bead with a spatial and temporal resolution in the nanometer and microsecond range, respectively. Due to the small trapping force constants, thermal position fluctuations of the probe are relatively large in comparison to the thermal motion of an AFM cantilever. However, these position fluctuations provide information about the local environment and specific interactions of the probe with molecules such as membrane proteins.

Within the few last years, the instrument turned out to be a powerful tool to study properties of the plasma membrane of intact cells at the nanometer scale. For instance, the diffusion of membrane components could be observed over minutes at high spatial and temporal resolutions. For the first time, the diffusion coefficient measured locally in the plasma membrane of an intact cell agreed well with previous measurements for lipid model membranes, thus providing new ways to characterize membrane structures with unknown properties, such as lipid rafts. Furthermore, the technique can be used to determine the elasticity of the lipid bilayer and the binding properties of membrane components to the cytoskeleton.

## Introduction

The Atomic Force Microscope (AFM) [1] allows to study non-conducting materials under ambient conditions and/or in solution. It was considered to be the ideal tool for physical studies of live biological specimens [2], soon after its invention living cells were imaged [3] and dynamic processes occurring at the cell membrane were examined [4]. However, the rough surface of a cell often prevents the tip of a mechanical cantilever from following fine topographic details. Furthermore, forces of several tens of piconewtons are necessary for stable imaging which can have the detrimental effect of deforming soft cellular structures, such as the plasma membrane. Only stiff structures, such as the cytoskeleton, are visible when imaging, whilst imaging inside cells is impossible due to the mechanical connection to the imaging tip. Therefore, a scanning probe microscope without a mechanical connection to the tip and working with extremely small loading forces is desirable. Such an instrument, the Photonic Force Microscope (PFM), has been developed at the European Molecular Biology Laboratory (EMBL) in Heidelberg during the last few years.

## Experimental Details

### Instrumentation

In the PFM the mechanical cantilever of the AFM is replaced by the 3-D trapping potential of a laser focus [5]. The ability to trap small particles with high stability was first described 1986 by Ashkin [6]. In the PFM a submicrometer-sized particle, e.g. a latex, glass or metal bead is used as a tip. The difference in the refractive index of the medium and the bead, the diameter of the bead, the laser intensity and the intensity profile in the focal volume, determine the strength of the trapping potential. Depending on the application, the potential is most easily adjusted by changing the laser power. In effect, the spring constant of the potential is two

to three orders of magnitude softer than that of the softest commercially available cantilevers.

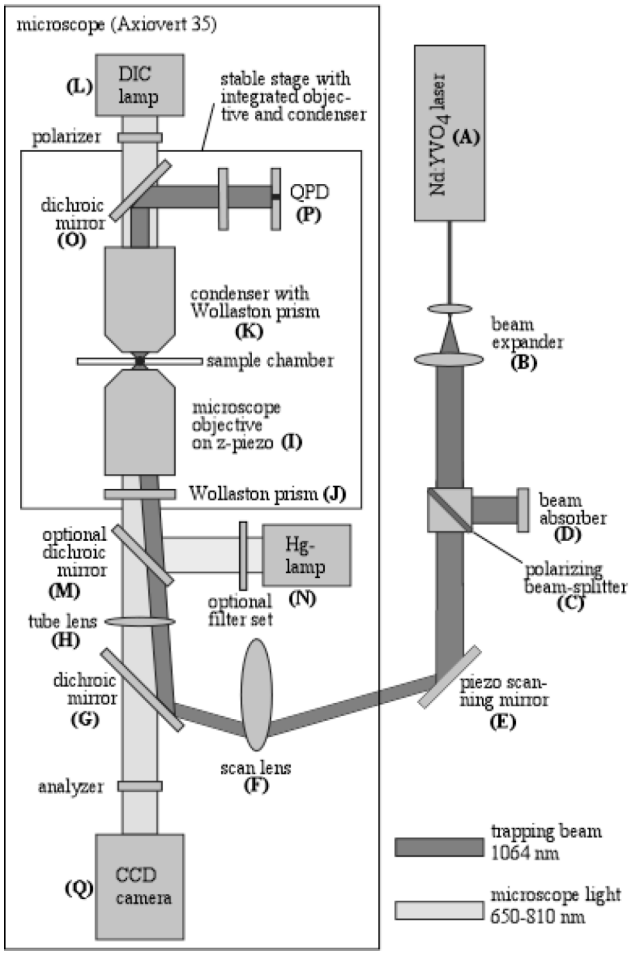


**Fig. 1**. *Scheme of the PFM: The trapping beam is emitted by a diode-pumped Nd:$YVO_4$ laser* (A) *(wavelength: 1064 nm, T20-B10-106Q, Spectra Physics, Germany) with a maximum power of 4 W in continuous wave mode. To achieve the high-intensity gradient necessary for a high trapping efficiency, the back-aperture of the focussing device is overilluminated. This is accomplished by adapting the effective diameter of the laser beam with a beam expander* (B). *For stability purposes the laser runs at high power and the intensity in the focus is regulated by a polarizing beam splitter* (C). *The beam is deflected onto a scanning mirror* (E), *mounted on a piezo scanner that can tilt around two axis (PSH2zNV, power supply: ENV 400/1, Piezosysteme Jena, Germany). The scan optics allows a lateral translation of the laser focus in the object plane of 3.9 µm. Inside the microscope, the beam is directed by a dichroic mirror* (G) *through the tube lens* (H) *onto the high numerical aperture (NA) oil-immersion objective lens (Neofluar 100x, NA = 1.3, Zeiss)* (I). *The objective lens is mounted on a piezoelectric actuator (PI-Foc, P721.00, Physik Instrumente, Germany) permitting the positioning of the laser focus along the optical axis over a range of 100 µm. The PI-Foc and the scanning arrangement serve as 3-D manipulators for the trapped object. The standard differential interference contrast (DIC) equipment includes a Wollaston prism* (J) *and a second one within the condenser* (K). *The DIC illumination* (L) *used here is restricted to a wavelength of about 700 nm. Optionally a dichroic mirror* (M) *and a Hg-lamp* (N) *can be placed together with a filter set into the light path in order to use fluorescence microscopy simultaneously. The laser light scattered by a trapped particle and the unscattered light are collected by the condenser lens* (K) *and projected onto the quadrant photodiode* (P) *(S5981, Hamamatsu, Japan) by a second dichroic mirror* (O) *(DELTA Lys. & Optics, Denmark).*

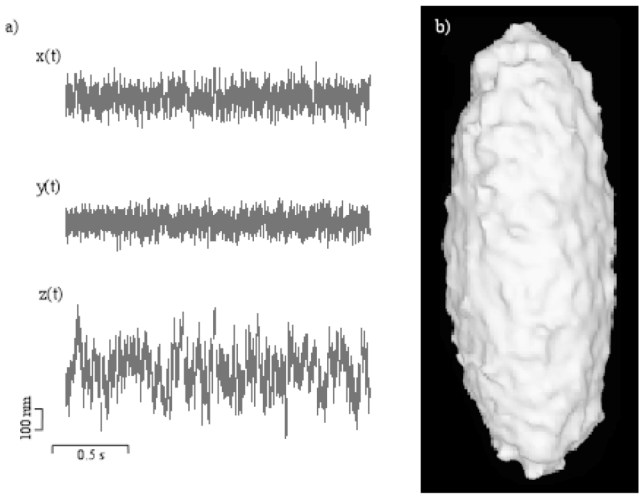


**Fig. 2.** *3-D position fluctuation analysis applying Boltzmann statistics.* **(a)** *Typical 3-D position fluctuation recordings of an optically trapped bead (430 nm in diameter) at low laser power in aqueous solution 2 µm from the coverslip surface. The sampling rate was 25 kHz. The peak-to-peak fluctuations have a maximum of 200 nm in the lateral directions (x, y) and 500 nm along the optical axis (z).* **(b)** *3-D energy isosurface (≈5 $k_BT$ above the global minimum) of the trapping potential calculated from 3-D position histograms using the data shown in* **(a).**

The PFM contains two position-sensing systems to determine the position of the trapped sphere relative to that of the potential minimum. The first sensor records the fluorescence intensity emitted by fluorophores inside the trapped sphere, which are excited by the trapping laser via a two-photon process. The fluorescence intensity provides an axially sensitive position signal with millisecond resolution [7]. The second sensor is based on the interference of the forward scattered light from the trapped particle with the unscattered laser light at a quadrant photodiode [8]. This provides a fast three-dimensional recording of the particle's position, and is most sensitive perpendicular to the optical axis. The position of the bead can be measured with a spatial resolution of better than one nanometer at a temporal resolution in the microsecond range. Depending on the application, either one or both of these detection systems can be used.

At room temperature the thermal position fluctuations of the trapped bead in weak trapping potentials reach several hundred nanometers. At first glance these fluctuations seem to be disturbing noise that limits the resolution. However, due to the speed and resolution of the position sensor based on the forward-scattered light detection, the fluctuations of the bead can be tracked directly, opening new ways to analyzing the interaction of the bead with its environment.

The PFM (Fig.1) development is based on an inverted optical microscope with a high numerical aperture objective lens providing a high resolution optical image of the investigated structures. The laser light is coupled into the microscope using techniques known from laser scanning microscopy and is focussed by the objective lens into the specimen plane. A 1064 nm Nd:$YVO_4$ laser is used since neither water nor biological material have significant absorption at this wavelength. A dichroic mirror behind the condenser deflects the laser light onto the quadrant photodiode. The difference between the left and right half of the diode provides the x-, the difference between upper and lower half the y-, and the sum signal the z-position [8]. For displacements small relative to the focal dimensions, the signals change linearly with the position of the bead in the trap.

The trapped particle acts as a Brownian particle in a potential well and its position distribution is therefore described by the Boltzmann-distribution. Such distributions p(r) are readily measured with the high spatial and temporal resolution available to the PFM. Thus allowing for the calibration of the three-dimensional trapping potential E(r) without any further knowledge but the temperature, using [9]

$$E(r) = -k_B T * \ln p(r) + E_0.$$

A precision of one-tenth the thermal energy $k_B T$ is achieved with a sufficient number of statistically independent position readings. Figure 2 shows a typical isoenergy surface of the trapping potential at ≈5 $k_B T$.

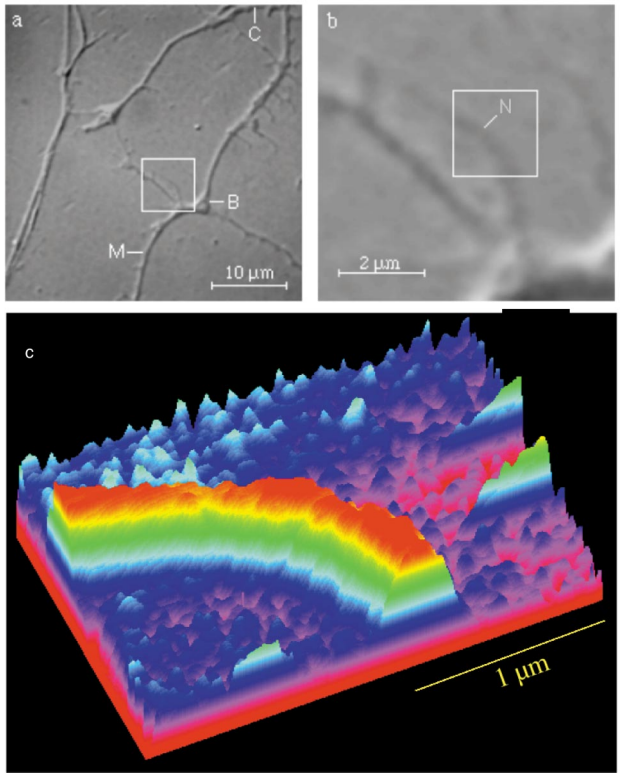


**Fig. 3.** *PFM imaging using a 200nm, fluorophore labelled latex bead and the two-photon fluorescence as position sensor. Optical DIC (a, b) and PFM (c) images of a small neurite (N) growing at a branching point (B) from a major neurite (M) of a glutaraldehyde fixed rat hippocampal neuron. The PFM image was acquired in constant height mode, with a loading force of smaller than 5pN (recording time about 30s).*

## Imaging

Scanning either the laser focus or the sample, the PFM can be used in a manner similar to the AFM to image surface topographies. The applied forces range from a few piconewtons down to fractions of one piconewton. The size of the smallest distinguishable structure is given by the diameter of the sphere, which can be some ten nanometers for metal beads or several hundreds of nanometers for latex or glass beads. Figure 3 shows an image of a neuronal dendrite obtained operating the PFM in constant height mode with a maximal force of about 1 pN using a latex bead with a diameter of ≈200 nm. Beside the constant height mode, other imaging modes known from AFM can be implemented using a feedback loop. Furthermore, due to the large thermal fluctuations of the bead a new imaging mode becomes possible with the PFM by observing the spatial distribution of the thermal fluctuations of the bead, which avoids stationary objects. In this way it is possible, to image for example the 3-D structure of polymer networks. Additionally, detailed information about the interaction potential between the bead and the surface of the objects

imaged can be obtained. At present, PFM imaging of biological material is limited by non-specific adhesion events between the bead and the sample, which can lead to the loss of the probe due to the weak forces applied. Although there seems to be no general strategy to prevent non-specific adhesion to complex biological material, it is still possible to achieve specific binding to membrane structures for a limited time as will be shown below (Fig. 5).

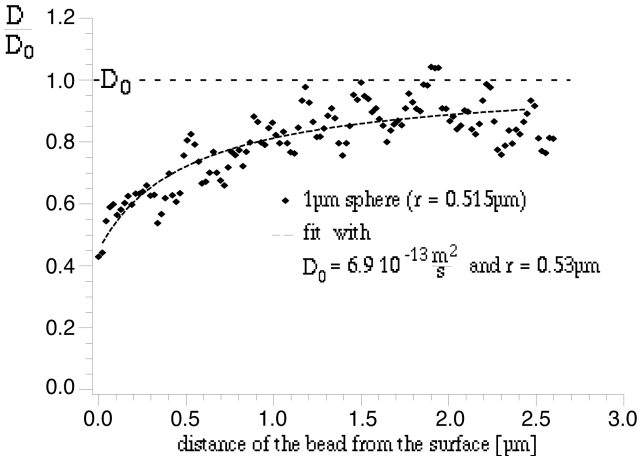


**Fig. 4.** *Local viscosity measurement. Decrease of the diffusion coefficient of a sphere approaching a surface measured for a polystyrene sphere with r=515nm using the PFM. The dotted line shows the theoretical prediction by Happel and Brenner fitted for r=530nm and a free solution diffusion constant of D=6.9 $10^{-13}m^2/s$.*

## Local Viscosity Measurements

The motion of a thermally fluctuating particle in a harmonic potential like that of the laser trap is to a certain level characterized by an exponentially decaying position autocorrelation function with a characteristic autocorrelation time $\tau=\gamma/\kappa$, where $\gamma$ denotes the viscous drag on the sphere and $\kappa$ the force constant of the optical trap. Thus, the local viscous drag and the diffusion coefficient $D = k_BT/\gamma$ of a sphere in a harmonic potential can be calculated from the measured autocorrelation time of the motion and stiffness of the potential [10]. The stiffness of the trapping potential is determined as described before for the calibration of the laser trap. To measure diffusion coefficients with a statistical error smaller than ten percent, the observation interval must be in the order of 1000 times longer than the autocorrelation time. Hence, the motion of the bead limits the temporal resolution of the viscosity measurement, and not the bandwidth of the detection system. Near surfaces, e.g. glass surfaces or cell membranes, the diffusion is reduced because of the spatial confinement (Fig. 4) [11]. Within an obstacle free lipid bilayer, diffusion has been described by Saffman and Delbrück [12] using a hydrodynamic model treating the bilayer as a continuum and assuming weak coupling to the surrounding liquid medium. The viscous drag $\gamma_m$ on a cylindrical particle with radius r in a homogeneous lipid bilayer of thickness h is: $\gamma_m = 4\pi\eta_m h/(\ln(\eta_m h/\eta_w r)-\varepsilon)$, where $\eta_w$ denotes the viscosity of the surrounding fluid, $\eta_m$ the viscosity of the lipid bilayer, and $\varepsilon$ the Euler constant. This approximation is valid for proteins with radii large compared to the size of the lipid molecules and for $\eta_m >> \eta_w$, which is true for cellular membranes. Thus, the membrane viscosity can be determined by binding a bead to a membrane structure of known diameter and measuring the total viscous drag on the bead as described above. Such measurements can be performed with a temporal resolution of 0.3 s and within areas of 100 nm in diameter.

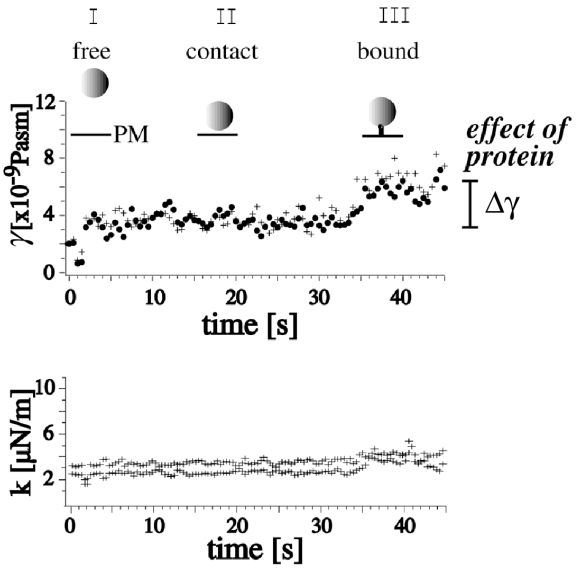


**Fig. 5.** *The viscous drag $\gamma$ (A) and the lateral spring constant $\kappa$ (B) during a typical experiment in which an antibody coated sphere (e.g. polyclonal anti-PLAP, sphere radius r=100nm) was brought close to the plasma membrane and held there until the antibody bound to the membrane protein ("+" x- and "•" y-direction). The traces show three regions corresponding to the reference measurement away from the surface (I), the diffusion near the plasma membrane (II) and after binding to the membrane protein (III). The lateral confining potential $\kappa$(B) remained unchanged during the entire experiment, whereas the lateral viscous drag $\gamma$ showed a clear chang e upon the antibody binding.*

## Local Viscous Drag of Single Membrane Components

Figure 5 depicts a typical measurement of the lateral viscous drag and spring constant of the trapping potential plotted against time for an experiment performed on the plasma membrane of a $PtK_2$ cell. The measured viscous drag $\gamma$ is the sum of the Stokes drag of the sphere $\gamma_s = 6\pi\eta_w r$ and the viscous drag $\gamma_m$ of e.g. a single protein in the lipid bilayer. The Stokes drag of the sphere near the cell membrane increases due to the confinement and must be corrected for the calculation of $\gamma_m$. The observation of the strength of the lateral potential ensures that the observed membrane component does indeed diffuses freely.

Using the PFM technique on a single transmembrane protein of known size it is possible to determine the membrane viscosity in living cells in areas of about 100 nm in diameter [13]. Once the membrane viscosity has been obtained, the PFM technique allows one to determine the diameter of other membrane structures and to monitor it continuously for several minutes. We performed such experiments to determine the size of membrane structures called "rafts" [13]. Lipid rafts are involved in the polarized sorting of proteins [14] and cellular signalling [15]. According to our study in the plasma membrane of fibroblast-like cells, these structures are indeed quite stable in the time-scale of minutes [15], thus justifying the model of “rafts” as lipid-protein complexes floating raft-like in the membrane [16]. Their diameter was determined to be about 50 nm.

In summary, the PFM has proven to be a powerful tool for the study of biophysical properties of plasma membranes as well as the interaction of single molecules or complexes of molecules within a membrane. Future applications of the PFM will cover a wide range from 3-D *in vivo* imaging of biological samples to a detailed investigation of single molecule properties.

## References

[1] G. Binnig, C.F. Quate and Ch. Gerber, Phys. Rev. Lett. **56**, 930 (1986)
[2] B. Drake, C.B. Prater, A.L. Weisenhorn, S.A.C. Gould, T.R. Albrecht, C.F. Quate, D.S. Cannell, H.G. Hansma and P.K. Hansma, Science **243**, 1586 (1989)
[3] W. Häberle, J.K.H.Hörber and G. Binnig, J. Vac. Sci. Tech., **B9**, 1210 (1991)
[4] J.K.H. Hörber, W. Häberle, F. Ohnesorge, G. Binnig, H.G. Liebich, C.P. Czerny, H. Mahnel and A. Mayr, Scanning Microscopy **6** (4), 919 (1992)
[5] E.-L Florin, A. Pralle, J.K.H. Hörber, and E.H.K. Stelzer, J. Stru. Biol. **119**, 202 (1997)
[6] A. Ashkin, Opt. Lett. **11**, 288 (1986)
[7] E.-L Florin, J.K.H. Hörber, and E.H.K. Stelzer, Appl. Phys. Lett. **69**, 446 (1996)
[8] A. Pralle, M. Prummer, E.-L. Florin, E.H.K. Stelzer and J.K.H. Hörber, Micr. Res. and Tech. **44**, 378 (1999)
[9] E.-L. Florin, A. Pralle, E.H.K. Stelzer and J.K.H. Hörber, Appl. Phys. A **66**, S75 (1998)
[10] A. Pralle, E.-L. Florin, E.H.K. Stelzer and J.K.H. Hörber, Appl. Phys. A **66**, S71 (1998)
[11] J. Happel and H. Brenner, Low Reynolds number hydrodynamics, Prentice Hall, New Jersey (1965)
[12] P.G. Saffman and M. Delbrück, Proc. Natl. Acad. Sci. USA **72**, 3111 (1975)
[13] A.Pralle, P.Keller E.-L. Florin, K. Simons and J.K.H. Hörber, J. Cell Biol. **148** (5), 997 (2000)
[14] P. Keller and K. Simons, J. Cell Biol. **140**, 1357 (1998)
[15] T.P. Stauffer and T. Meyer, J. Cell Biol. **139**, 1447 (1997)
[16] K. Simons and E. Ikonen, Nature **387**, 569 (1997)